Cellular uptake of fatty acids driven by the ER-localized acyl-CoA synthetase FATP4

Katrin Milger[1], Thomas Herrmann[1], Christiane Becker[1], Daniel Gotthardt[1], Jelena Zickwolf[1], Robert Ehehalt[1], Paul A. Watkins[2], Wolfgang Stremmel[1,*] and Joachim Füllekrug[1,*,‡]

[1]Department of Gastroenterology, Im Neuenheimer Feld 345, University of Heidelberg, 69120 Heidelberg, Germany
[2]Kennedy Krieger Institute, 707 N. Broadway, Baltimore, MD 21205, USA

*Shared last authorship
‡Author for correspondence (e-mail: Joachim.Fuellekrug@med.uni-heidelberg.de)

Accepted 14 September 2006
Journal of Cell Science 119, 4678-4688 Published by The Company of Biologists 2006
doi:10.1242/jcs.03280

Summary

Long-chain fatty acids are important metabolites for the generation of energy and the biosynthesis of lipids. The molecular mechanism of their cellular uptake has remained controversial. The fatty acid transport protein (FATP) family has been named according to its proposed function in mediating this process at the plasma membrane. Here, we show that FATP4 is in fact localized to the endoplasmic reticulum and not the plasma membrane as reported previously. Quantitative analysis confirms the positive correlation between expression of FATP4 and uptake of fatty acids. However, this is dependent on the enzymatic activity of FATP4, catalyzing the esterification of fatty acids with CoA. Monitoring fatty acid uptake at the single-cell level demonstrates that the ER localization of FATP4 is sufficient to drive transport of fatty acids. Expression of a mitochondrial acyl-CoA synthetase also enhances fatty acid uptake, suggesting a general relevance for this mechanism. Our results imply that cellular uptake of fatty acids can be regulated by intracellular acyl-CoA synthetases. We propose that the enzyme FATP4 drives fatty acid uptake indirectly by esterification. It is not a transporter protein involved in fatty acid translocation at the plasma membrane.

Supplementary material available online at
http://jcs.biologists.org/cgi/content/full/119/22/4678/DC1

Key words: Fatty acid uptake, FATP4, Endoplasmic reticulum, Acyl-CoA synthetase

Introduction

Cellular uptake of long-chain fatty acids is the requirement for their utilization as metabolic fuels, building blocks and signaling molecules. Transport of small metabolites like glucose has been shown to rely on membrane proteins creating a channel in the plasma membrane through which molecules enter the intracellular environment. However, the molecular mechanism for the transport of fatty acids across the plasma membrane has remained unresolved. Although there is general agreement that fatty acids can principally be taken up by passive diffusion across the lipid bilayer, the extent and significance of this process is a matter of considerable debate (Black and DiRusso, 2003; Hamilton et al., 2002; Stahl et al., 2001; Zakim, 2000). Several membrane-associated proteins have been put forward to act as fatty acid transporters. How and to which degree these proteins facilitate fatty acid uptake across the plasma membrane (or if they are necessary at all) is highly controversial too. This is also reflected by the very different molecular properties of the three main mammalian candidate fatty acid transporters implicated, none of which displays the topology of a classical membrane channel. The evidence for and against a role as a fatty acid transporter for plasma-membrane-associated fatty-acid-binding protein (FABPpm), fatty acid translocase (FAT)/CD36 and the fatty acid transport protein (FATP) family has been reviewed extensively (Bonen et al., 2002; Hajri and Abumrad, 2002; Hamilton and Kamp, 1999; Stahl et al., 2001).

FATP1 and acyl-CoA synthetase long-chain family member 1 (ACSL1) were both identified based on their ability to enhance fatty acid uptake when overexpressed (Schaffer and Lodish, 1994). Subsequently a whole family of FATP proteins with tissue-specific expression patterns was described (Hirsch et al., 1998). FATP4 is the predominantly expressed FATP family protein in the mammalian gut and has been suggested to constitute the major intestinal fatty acid transporter (Stahl et al., 1999). Apart from the fatty acid uptake correlating with expression levels of FATP4, the evidence was based on the plasma membrane localization reported that would be required for a transporter function.

FATP4 and other FATP family proteins carry an acyl-CoA synthetase activity (Hall et al., 2003; Hall et al., 2005), which has led to substantial speculation about their role in fatty acid uptake. The possibility of an indirect contribution by intracellular trapping of fatty acids by esterification with CoA has been raised (Kalant and Cianflone, 2004; Pei et al., 2004). The subcellular localization to the plasma membrane has also been questioned (Garcia-Martinez et al., 2005; Steinberg et al., 1999b), but has been rejected on the grounds of possible mislocalization of overexpressed protein (Lewis et al., 2001; Stahl et al., 2001).

Interference with intestinal fatty acid uptake is one of the

key strategies in fighting obesity and associated dyslipidaemia, diabetes and hypertension (Bray and Tartaglia, 2000). We therefore sought to pinpoint the role of FATP4 in fatty acid uptake. We present extensive evidence that FATP4 is localized to membranes of the endoplasmic reticulum (ER). Moreover, by analyzing FATP4 localization and fatty acid uptake simultaneously at the single-cell level, we show that expression at the ER is sufficient to drive enhanced uptake of fatty acids. We propose that enzymatic activity of FATP4, the esterification of fatty acids with CoA, is the cause behind the correlation of FATP4 expression with fatty acid uptake. In line with this, the intracellular enzyme ACSL1 also enhances fatty acid uptake.

Results

Localization of FATP4

The physiological function of FATP4 is in lipid metabolism, and knockout (KO) mice studies have revealed an essential role for viability (Gimeno et al., 2003; Herrmann et al., 2003; Moulson et al., 2003). We then turned to elucidate the molecular role of FATP4 in the process of fatty acid uptake. FATP1, the best-characterized protein of the FATP family, was localized to the plasma membrane (Gargiulo et al., 1999; Schaffer and Lodish, 1994) but there are conflicting studies on FATP family proteins more consistent with an intracellular localization (Garcia-Martinez et al., 2005; Pei et al., 2004; Steinberg et al., 1999b). This prompted us to re-investigate the localization of FATP4.

FATP4 tagged with green fluorescent protein (GFP) localized intracellularly in a network-like ER pattern in a variety of different cell lines (HeLa, Caco-2, Ptk2, MDCK, COS). Shown are MDCK cells, which are stably transfected to exclude artificial ER accumulation due to transient overexpression (Fig. 1A). In HeLa cells, FATP4-GFP showed the same localization pattern as the coexpressed ER resident protein CaBP1 but was segregated from the plasma membrane marked by CD8 (Fig. 1B,C). An initial concern in our studies was that epithelial polarization might be required for proper localization of FATP4, and we therefore investigated terminally polarized MDCK cells by confocal laser scanning microscopy. Vertical sections showed that FATP4-GFP is present intracellularly, which is clearly different from the apical plasma membrane antigen gp114 (Fig. 1D). When MDCK cells were imaged in the plane where nuclei are prominent, FATP4-GFP almost looked like it could be localized to the plasma membrane. However, comparison with the lateral membrane marker p58 shows that FATP4-GFP is, in fact, present in the small cytoplasmic area between the nucleus and the membrane (Fig. 1E). FATP4-GFP is a functional protein because it enhanced oleate uptake when overexpressed (see below).

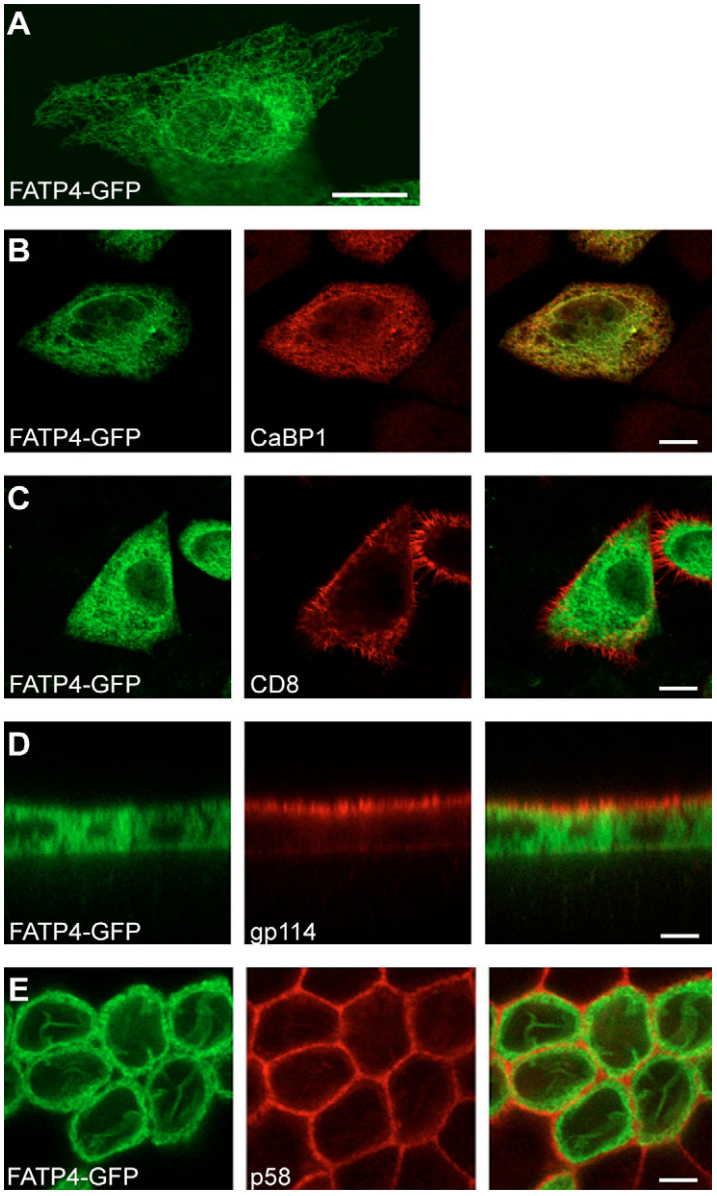

Fig. 1. Intracellular localization of FATP4-GFP. (A) Intracellular reticular localization of FATP4 in stably expressing MDCK cells. Shown is a single section obtained by confocal microscopy to demonstrate the reticular distribution clearly. (B) FATP4 colocalization with the ER marker protein CaBP1 in transiently transfected HeLa cells. (C) FATP4 comparison with a plasma membrane marker protein (CD8); transiently expressing HeLa cells. Only one confocal plane close to the bottom is shown. Bars, 10 μm. (D,E) Intracellular localization of FATP4 in terminally polarized MDCK cells. (D) The apical plasma membrane (side view) is stained with an antibody to gp114. (E) The lateral plasma membrane (midsection, one confocal plane only) is identified by p58. Note that FATP4-GFP is present between the plasma membrane and the nucleus, and not colocalizing with p58. Bars, 10 μm.

The localization of FATP4-GFP to the ER was an unexpected finding and would of course not support a transporter function of FATP4. Therefore, we decided to analyze the distribution of FATP4 in more detail.

Exogenous expression of wild-type (wt) FATP4 in tissue culture cells followed by immunofluorescence staining again showed a reticular network-like staining characteristic of the ER. Comparison with marker proteins for the ER and the plasma membrane (lysozyme-KDEL and ICAM-1-GFP, respectively) demonstrated ER localization but segregation from the plasma membrane (Fig. 2A,B). The ER localization of FATP4 was observed over a wide range of apparent expression levels and did not change after inhibition of protein synthesis.

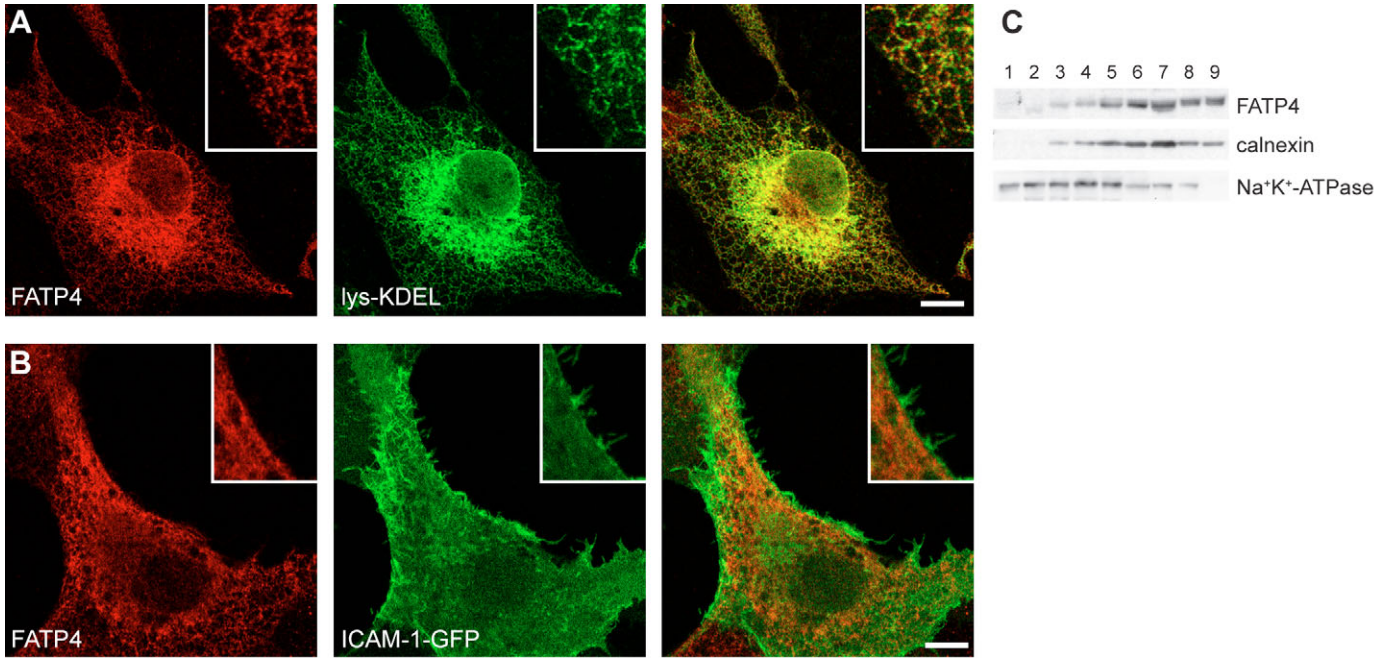

Fig. 2. Localization of wt FATP4. (A) Expression of FATP4 in COS cells. Lysozyme-KDEL (green) was cotransfected as an ER marker protein. Staining of the nuclear envelope and the reticular network-like pattern (inset) indicates ER localization. Both proteins clearly label the same structure but there is some microheterogeneity. Inhibition of protein synthesis using cycloheximide did not change the localization pattern of FATP4. Shown is a single confocal plane. Bar, 10 μm. (B) Coexpression of FATP4 and a plasma membrane marker protein (ICAM-1-GFP) in Vero cells. There is no significant overlap, which is especially evident at the edge shown in the magnified inset. Bar, 10 μm. (C) Codistribution of endogenous FATP4 with ER membranes after subcellular fractionation. A postnuclear supernatant was prepared from HeLa cells and analyzed by velocity-controlled density centrifugation on an Optiprep step gradient. Fractions were collected from top to bottom and analyzed by SDS-PAGE and western blotting. Calnexin and Na^+K^+-ATPase served as markers for the ER and the plasma membrane, respectively.

This suggests that the observed staining pattern reflects the steady-state localization of FATP4 in the ER and not an artifact caused by accumulation of newly synthesized protein.

Subcellular fractionation of tissue culture cells demonstrated that endogenous FATP4 is co-fractionating with heavy membranes marked by calnexin, a resident protein of the ER. The distribution of FATP4 was different from the light plasma membrane fractions marked by Na^+K^+-ATPase (Fig. 2C).

To confirm that our results using tissue culture cells correctly reflect the situation in vivo, we performed immunohistochemistry of mouse small intestine. Single stainings viewed at low magnification indicated that FATP4 is mainly localized above the nuclei of the enterocytes, oriented towards the lumen of the gut (Fig. 3A). This was not apical staining, however, because double immunohistochemistry demonstrated an intracellular cytoplasmic localization of FATP4 but no significant staining of the apical membrane marked by alkaline phosphatase (Fig. 3B). The specificity of the staining was confirmed by pre-incubation of the antibody with the peptide used for immunization. In addition, blotting of total lysate from the intestine of wt and KO mice gave only a signal for wt tissue (Fig. 3C).

Targeting of FATP4

Because of the controversial discussion on the localization of FATP family proteins, we sought to gain more insight into how FATP4 is localized to the ER. Sequence analysis of FATP4 indicated a stretch of hydrophobic amino acids close to the N-terminus probably forming a transmembrane domain (TMD). Other hydrophobic regions displayed a much lower probability and were not conserved among vertebrate FATP4 sequences (data not shown). In line with this, a mutant FATP4 (ΔN-F4) lacking the N-terminal region up to the end of the predicted TMD was found in cytosolic fractions (data not shown). To determine the membrane topology of FATP4, we extended the N-terminus with a short glycosylation tag derived from human rhodopsin (Bulbarelli et al., 2002). N-glycosylation was evidenced by an additional band of higher molecular mass and sensitivity towards endoglycosidase H (EndoH) (Fig. 4A). Therefore, the N-terminus of FATP4 is oriented towards the lumen of the ER. This is in agreement with the topology predicted by the positive-inside rule regarding the distribution of positively charged amino acids surrounding the TMD (Hartmann et al., 1989; von Heijne, 1989; Higy et al., 2004). In summary, all experimental data and theoretical analyses are consistent with a type III signal-anchor TMD topology of FATP4. A short N-terminal sequence is oriented towards the lumen of the ER, whereas the enzyme part of FATP4 is located cytoplasmically (Fig. 4B).

N-glycans become EndoH-resistant after being processed by α-mannosidase II in the Golgi complex. Glycosylated FATP4 remained EndoH-sensitive (Fig. 4A), suggesting that FATP4 is a protein resident of the ER. Moreover, unlike some cycling ER proteins, FATP4 is apparently not even transiently reaching the Golgi complex or other subcellular compartments of the secretory pathway.

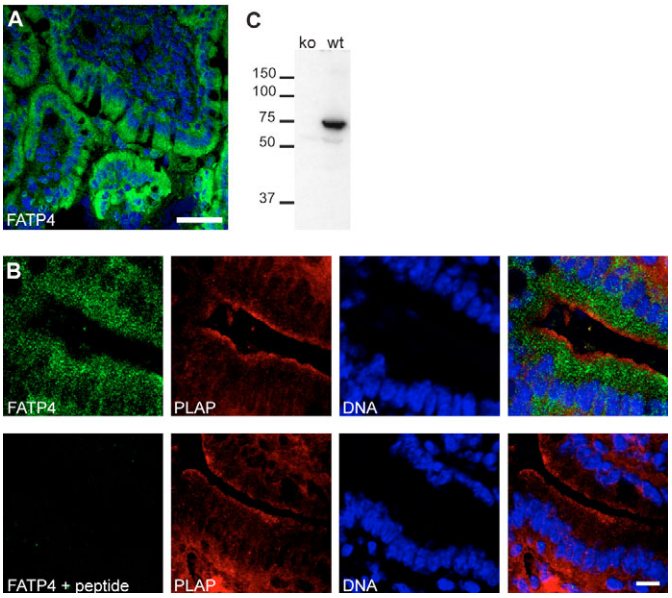

Fig. 3. Immunohistochemistry of mouse small intestine. (A) Overview of FATP4 distribution. FATP4 (green) is mostly above the nuclei (blue) and oriented towards the lumen of the gut. Intestinal villi are shown in midsection. Bar, 40 μm. (B) Comparison of FATP4 and an apical marker protein. Sections were labeled with affinity purified antibodies against FATP4 and a mouse monoclonal antibody against PLAP. Pre-incubation with the C-terminal peptide of FATP4 abolishes the cytoplasmic staining pattern of FATP4. Exposure times for sections were identical. Bar, 10 μm. (C) Analysis of intestinal lysates of embryos of wt and FATP4 KO mice. Equal amounts of total lysate (50 μg) were separated by SDS-PAGE and developed by western blotting. A strong band at 72 kDa indicates the presence of FATP4 in the wt but the absence in the intestine of KO mice. Molecular mass markers are indicated in kDa.

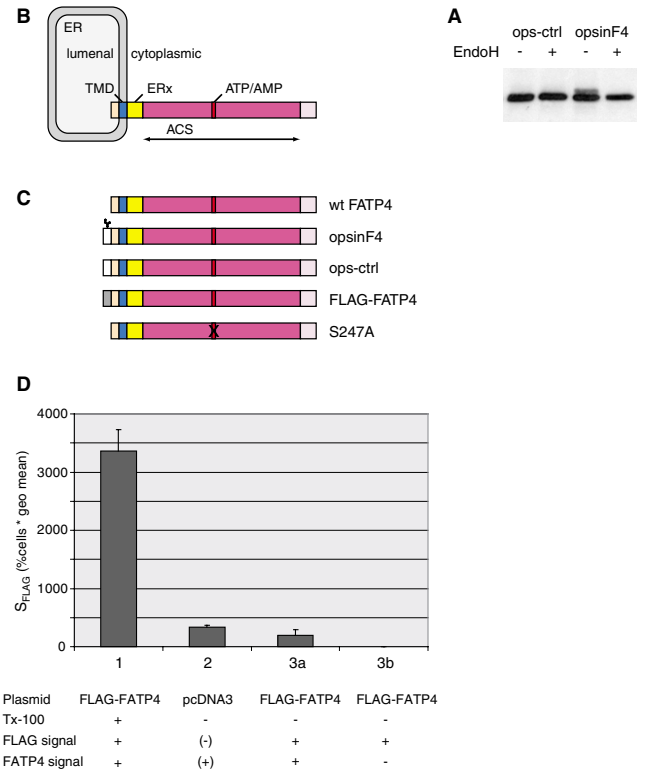

Fig. 4. Topology of FATP4. (A) Glycosylation analysis. HeLa cells were transfected with N-terminal-tagged FATP4 variants containing either consensus sites for N-glycosylation (opsinF4) or not (ops-ctrl). Membrane preparations were treated with EndoH as indicated. The upper band in the third lane marks an EndoH-sensitive glycosylation, suggesting that opsinF4 is restricted to the ER. (B) Proposed topology for FATP4. The N-terminus is located in the lumen of the ER. A single TMD is followed by the ERx domain. The acyl-CoA synthetase homology region (ACS) corresponds to the protein family of AMP-binding enzymes (pfam00501). (C) Overview of FATP4 mutant proteins. OpsinF4 contains an N-terminal extension allowing N-glycosylation. Ops-ctrl has two amino acid changes destroying the consensus sites for glycosylation. FLAG-FATP4 features an N-terminal epitope tag. S247A contains an inactivating point mutation in the AMP-binding region; serine 247 is changed to alanine. (D) Surface quantification of FLAG-FATP4 by FACS analysis. COS cells were transfected with FLAG-FATP4 or the control plasmid pcDNA3, and processed for FACS analysis either PFA fixed and TX-100 permeabilized (sample 1) or not permeabilized (samples 2, 3). The percentage of gated cells was multiplied with the geometric mean of the fluorescence signal derived from the FLAG antibodies to give the arbitrary value for the total signal (S_{FLAG}). (1) Expression of FLAG-FATP4 and permeabilization with TX-100 yields the maximum FLAG signal. (2) Cells transfected with pcDNA3 do not express the FLAG epitope; the remaining signal is because of unspecific binding. The FATP4 antibody gives a signal for endogenous protein. (3a) Cells transfected with FLAG-FATP4, not permeabilized. This signal is in the background range, and the cells were also positive for the internal antigen FATP4, revealing that the surface is leaky. (3b) This is a subpopulation of 3a and would represent cells with an intact surface that are positive for the FLAG signal but negative for FATP4. See also the Materials and Methods section for more details.

Although we could not find any FATP4 at the plasma membrane (Figs 1-3), the formal possibility remained that perhaps only a small fraction of FATP4 (below the threshold for detection by immunocytochemistry) is reaching the plasma membrane. This has been argued (Stahl et al., 2001), especially when the localization of FATP proteins was investigated after transient expression in tissue culture cells (Lewis et al., 2001; Steinberg et al., 1999a; Steinberg et al., 1999b). The extracytoplasmic N-terminus of wt FATP4 is short (19 amino acids) and not immunogenic; therefore we appended an epitope tag (FLAG) to enable surface quantification. FLAG-FATP4 expressed in COS cells behaved the same as wt FATP4 (localization to the ER and enhanced fatty acid uptake; data not shown). The immunofluorescence signal was evaluated on random microscopy sections; arbitrary values were 1.61±0.63 for permeabilized cells, –0.11±0.19 for unpermeabilized cells and 0.0±0.26 for control cells not expressing the FLAG epitope (not shown). For a more definitive surface quantification we applied fluorescence-activated cell scanning (FACS). Permeabilized cells gave a strong signal, but the amount of anti-FLAG antibody bound to the surface of the transfected cells was in the background range (Fig. 4D). Together with the FLAG antibody we applied our FATP4 antibody against the C-terminus which can only bind inside the cell regardless of where FATP4 is localized. Therefore, intact cells would have only a signal for the FLAG epitope (if any protein is present at the plasma membrane), whereas leaky cells damaged during

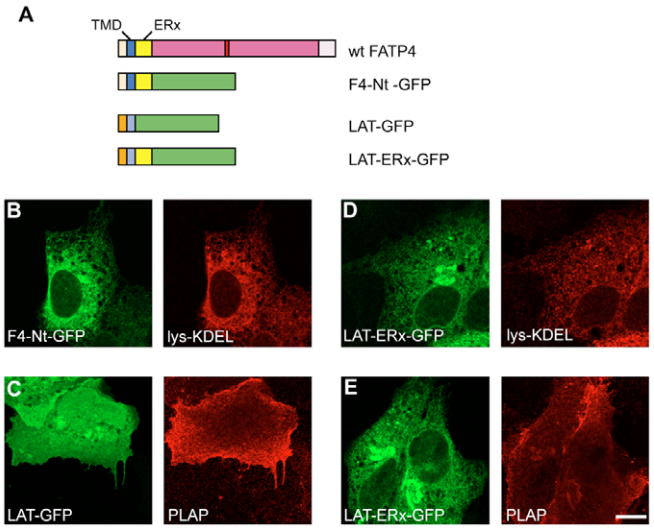

Fig. 5. Targeting of FATP4. (A) Domain architecture of GFP reporter proteins. F4-Nt-GFP contains the first 102 amino acids of mouse FATP4 followed by GFP. LAT-GFP comprises the N-terminal targeting domain (extracellular part, orange box; TMD, light-blue box) of LAT fused to GFP. LAT-ERx-GFP contains the ERx domain of FATP4 (amino acids 47-102, yellow box) inserted into LAT-GFP. (B) The N-terminus of FATP4 is sufficient for the ER localization. Vero cells were transiently transfected with plasmid F4-Nt-GFP and treated for 2 hours with the protein synthesis inhibitor cycloheximide before fixation. Localization to the ER is evidenced by co-distribution with the marker protein lysozyme-myc-KDEL. (C-E) Targeting mediated by the ERx domain. The reporter protein LAT-GFP is localized to the plasma membrane (C). (D,E) Insertion of the 56 amino acids of the ERx domain is sufficient to retain the corresponding LAT-ERx-GFP protein intracellularly. LAT-ERx-GFP is present in the ER (co-distribution with lysozyme-myc-KDEL; D) and in a perinuclear compartment, clearly different from the plasma membrane marked by PLAP (E). Bar, 10 μm.

the preparation would have a signal both for the FLAG epitope and the FATP4 C-terminus. In fact, when cells displaying the (background) FLAG signal were analyzed, all of them also showed a FATP4 signal (Fig. 4D). In conclusion, no significant signal was found for FLAG-FATP4 at the cell surface.

To identify targeting regions within FATP4 we used a domain-swapping approach employing GFP as a reporter protein. A fusion protein containing only the first 102 amino acids of FATP4 (F4-Nt-GFP) localized to the ER like wt FATP4 (Fig. 5B), suggesting that the relevant sorting information is contained in the N-terminus and in neither the ACS homology region nor the C-terminus. A different construct containing GFP directly after the TMD was not efficiently expressed (data not shown). Between the TMD of FATP4 and the ACS homology region lies a 60-amino-acid stretch of unknown function that we provisionally termed the ERx domain. LAT (linker of activation of T cells) has a type III signal-anchor TMD topology like FATP4, and an N-terminal LAT-GFP fusion protein (Tanimura et al., 2003) was localized at the plasma membrane (Fig. 5C). Strikingly, when the ERx domain of FATP4 was introduced into LAT-GFP, this protein did not reach the plasma membrane but was retained in the ER and a perinuclear compartment, probably the Golgi complex (Fig. 5D,E). Since the LAT-ERx-GFP fusion protein, although clearly intracellular, is not as efficiently localized to the ER as the F4-Nt-GFP protein, this could indicate that there is additional targeting information in the TMD or even the luminal tail of FATP4.

Localization and targeting of ACSL1

Both the FATP family proteins and the long-chain fatty acid acyl-CoA synthetases of the ACSL family are capable of catalyzing the esterification of CoA with fatty acids. Contrary to FATP family proteins, the best-characterized ACSL family member ACSL1 (Coleman et al., 2000) is considered to be devoid of a fatty-acid-transport function (Gargiulo et al., 1999). Therefore, we initially intended to compare ACSL1 (enzyme)

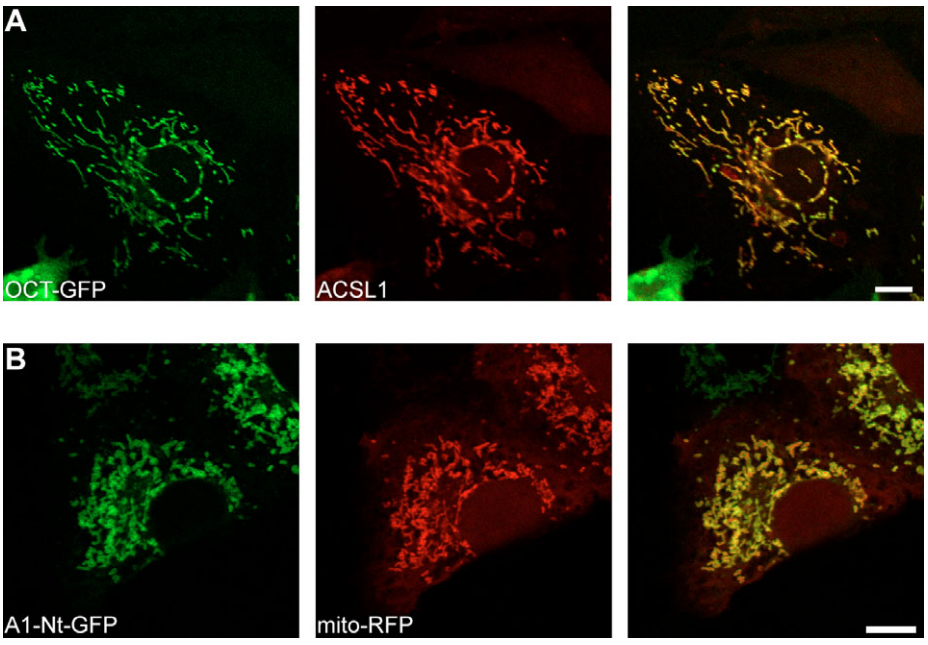

Fig. 6. Localization and targeting of ACSL1. (A) Epitope-tagged ACSL1 was co-expressed with a mitochondrial marker protein (OCT-GFP) in Ptk2 cells. One representative section obtained by confocal microscopy is shown. Bar, 10 μm. (B) A1-Nt-GFP contains the 66 N-terminal amino acids of ACSL1 followed by GFP. Overlap with a mitochondrial red fluorescent protein (RFP) coexpressed in Vero cells demonstrates that the N-terminus of ACSL1 is sufficient for targeting. Bar, 10 μm.

with FATP4 (enzyme, transporter or both) to gain more insight into the role of FATP4 during uptake of fatty acids.

ACSL1 localization in epithelial-like tissue culture cells was intracellular but different from FATP4 when investigated by light microscopy. Colocalization with a marker protein showed that ACSL1 is present on mitochondrial membranes in these cells (Fig. 6A; see also supplementary material). In confirmation of this, the N-terminus of ACSL1 was sufficient to target a GFP fusion protein to mitochondria (Fig. 6B).

Analysis of fatty acid uptake

Having established the localization of FATP4 and ACSL1, we then looked for an experimental system in which we could correlate localization with fatty acid uptake. This would provide evidence that FATP4 really is functionally relevant when localized at the ER membrane.

Transient expression of FATP4 and ACSL1 in COS cells was followed by a short-time incubation with the fluorescent long-chain fatty acid B_{12}-FA (Bodipy 3823) and processing for microscopy. This enabled us to investigate fatty acid uptake and localization simultaneously, in the same cell. Cells expressing FATP4 in a distinct reticular ER pattern were also the cells taking up more fluorescent fatty acid than their untransfected counterparts (Fig. 7). ACSL1-expressing cells were also more efficient than nontransfected cells.

This method allowed us to correlate the localization pattern directly with the uptake of the fluorescent fatty acid on a qualitative level. We then sought to gain more quantitative data by analyzing a larger number of individual cells by FACS. After FATP4 transfection a population of cells with higher uptake values for the fluorescent fatty acid was observed (data not shown). To be able to correlate the amount of overexpressed FATP4 or ACSL1 with the amount of fluorescent fatty acid taken up, we co-transfected a soluble fluorescent molecule (tdimer) (Campbell et al., 2002). The standard histogram or dot-plot output of the FACS software again confirmed that overexpression enhanced fatty acid uptake, but a correlation analysis was only possible after transformation of the data by a new spreadsheet method (Tzircotis et al., 2004). FATP4 and ACSL1 expression of individual cells as indicated by the cotransfected tdimer correlated very well with the amount of fatty acid taken up (Fig. 8A). Importantly, a mutant FATP4 that carries a single amino acid substitution (S247A) interfering with the acyl-CoA synthetase activity (Stuhlsatz-Krouper et al., 1998) did not show significant uptake of fatty acid above background.

For both purified FATP4 and ACSL1 it has already been shown that they carry an acyl-CoA synthetase activity (Hall et al., 2005). We confirmed that under our conditions both enzymes are functional by measuring acyl-CoA synthetase activity after transient expression in tissue culture cells using oleate as a substrate (Fig. 8B). Acyl-CoA synthetase activity was also dependent on the level of FATP4 expression (data not shown). The 'enzyme-dead' S247A-FATP4 mutant did not show significant activity, although expression and localization were indistinguishable from the wt protein.

We also confirmed with a physiological substrate (oleate) that overexpression of FATP4 or ACSL1 enhanced fatty acid uptake (Fig. 8C). As before, the transfected cells showed a clear ER or mitochondrial pattern, respectively. ACSL1 is slightly more efficient than FATP4 regarding oleate uptake but

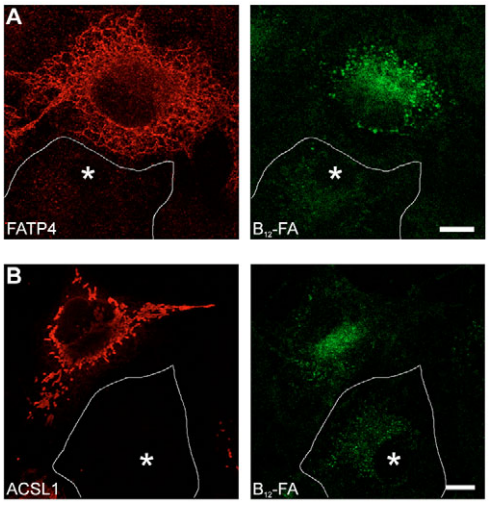

Fig. 7. Simultaneous analysis of expression, localization and fatty acid uptake. FATP4- (A) or ACSL1 (B)-transfected COS cells were incubated for 2 minutes with 20 μM of the fluorescent fatty acid analog B_{12}-FA, fixed and processed for indirect immunofluorescence. Untransfected cells (outlined, nuclei marked with an asterisk) indicate the background level of fluorescent fatty acid uptake. The distinct reticular ER pattern of FATP4 demonstrates that intracellular localization is sufficient to drive enhanced uptake of fatty acids. Cells expressing ACSL1 localized to mitochondria also show higher B_{12}-FA uptake than untransfected cells. Bar, 10 μm.

for the fluorescent fatty acid efficiencies were reversed (compare Fig. 8C with 8A). This is probably because of different substrate specificities for these enzymes (Hall et al., 2005). The enhanced oleate uptake was not accompanied by an accumulation of free oleate in the cells. Only 5-8% of oleate remained unesterified, which is in line with other reports (Guo et al., 2005; Pohl et al., 2002; Stremmel and Berk, 1986).

In summary, an intracellular localization of FATP4 or ACSL1 is sufficient to enhance cellular uptake of fatty acids. The acyl-CoA synthetase activity is necessary for this indirect way of regulating fatty acid uptake.

Discussion

FATP4 has been proposed to constitute the long-sought intestinal fatty acid transporter (Stahl et al., 1999), and is currently being classified as a member of the solute carrier family 27 (fatty acid transporter; HUGO Gene Nomenclature Committee). When it became evident that this protein and the other FATP family members have acyl-CoA synthetase activity, we and others began to express some doubt about the true function of this protein family (Coe et al., 1999; Stremmel et al., 2001; Watkins et al., 1999). Guided by our initial findings of an ER localization of FATP4-GFP, we chose the most straightforward strategy to determine whether FATP4 is a plasma membrane fatty acid transport protein: to analyze the subcellular localization.

We found no evidence for a plasma membrane localization of FATP4 using several different immunocytochemical approaches in various model systems. Moreover, independent methods of biochemical analysis by subcellular fractionation, processing of N-glycans and surface quantification were also consistent with a localization of FATP4 in the ER. We even

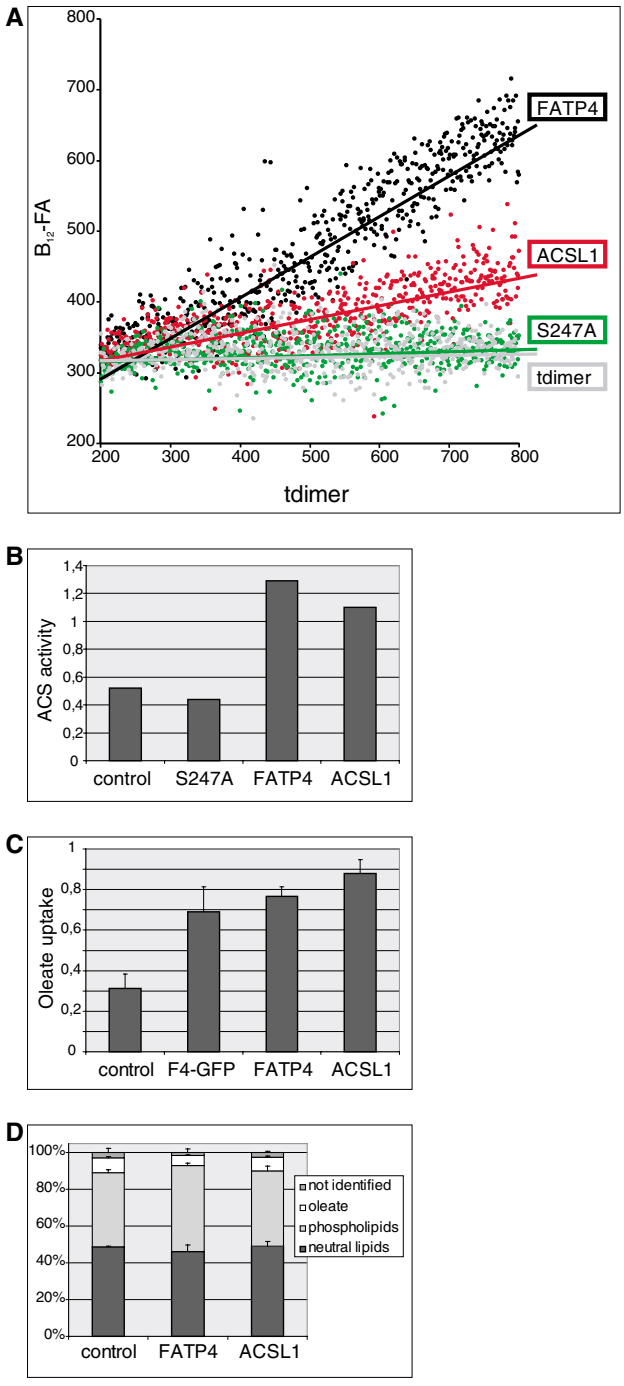

Fig. 8. Analysis of fatty acid uptake. (A) FACS of COS cells cotransfected with the red fluorescent tdimer protein. This enables the correlation of expression with the amount of the fluorescent fatty acid analog B_{12}-FA taken up. Both FATP4 (r=0.93) and ACSL1 (r=0.71) enhance fatty acid uptake depending on their relative level of expression. The S247A mutant FATP4 protein (serine 247 critical for AMP binding changed to alanine) is not significantly different from control cells expressing only tdimer. (B) Acyl-CoA synthetase activity (in pmol oleoyl-CoA/minute/μg protein) determined from the lysates of COS cells. Controls for endogenous ACS activity are transfected with empty plasmid (pcDNA3) or the S247A-FATP4 mutant. The ACS activities should be considered qualitative rather than absolute because ACSL1 and FATP4 showed inverse susceptibilities towards the detergent used for solubilization (see Materials and Methods). (C) Oleate uptake of COS cells (pmol oleate/μg protein after 5 minutes). (D) Lipid analysis after oleate uptake. After 5 minutes, 87-92% of oleate is already metabolized into phospholipids and neutral lipids. The level of the remaining free oleate is only 5-8%.

identified a new targeting-retention motif within FATP4 that is sufficient to retain a reporter protein.

Expression of FATP family proteins has been suggested to lead to an intracellular accumulation or aggregation that would prevent transport to the plasma membrane (Lewis et al., 2001; Stahl et al., 2001). Apart from demonstrating that endogenous FATP4 is localized intracellularly in mouse intestine enterocytes, the single-cell B_{12}-FA assays (Fig. 7) provide a strong independent line of evidence: by correlating expression, localization and qualitative fatty acid uptake simultaneously in the same cell, we showed that a plasma membrane localization is not required. Indeed, a localization of FATP4 at the ER or ACSL1 at mitochondria is sufficient to drive enhanced uptake of fatty acids.

We have used affinity-purified antibodies, double labeling with marker proteins and high-resolution confocal microscopy in various cell lines and model systems. Is there any chance we could have missed a plasma membrane localization? Sometimes an antibody is more specific for one localization compared with another, as reported for caveolin-1 (Luetterforst et al., 1999). However, the FATP4-GFP fusion protein shows the same ER localization, ruling out that our antibody is missing a subpopulation of FATP4 molecules. GFP-tagged FATP4 was functional when assayed for enhanced oleate uptake. In the initial study on FATP4, immunocytochemistry was also done (Stahl et al., 1999). In fact, the images obtained by light microscopy appear very similar to our overview section (Fig. 3A). We have now looked with higher magnification, and have also used an apical membrane marker. This shows that FATP4 is present in the cytoplasmic area (Fig. 3B). Since the nuclei of enterocytes are close to the basal membrane and most of the cytoplasmic area is above the nuclei, any cytosolic or cytoplasmic protein creates the appearance of being oriented to the apical side at low resolution. By immunoelectron microscopy, strong labeling was observed for microvilli and unidentified membranous structures (Stahl et al., 1999). Since no controls were mentioned and the antibody was not affinity-purified, it is difficult for us to evaluate this retrospectively. Sometimes, specificities differ for a given antibody depending on the technique.

ACSL1 has been localized to the ER and mitochondrial-associated membrane by subcellular fractionation of rat liver (Lewin et al., 2001). In our hands, the predominant localization of the epitope-tagged ACSL1 expressed in epithelial-like tissue culture cells was on mitochondria. Differential splicing or cell-specific localization could explain these differences. Although we observed that the N-terminus of ACSL1 was sufficient for targeting GFP to mitochondria, we could not investigate the localization of wt protein. Although we did see some ER staining in highly expressing COS cells, we never observed a plasma membrane localization for ACSL1 (as reported for adipocytes) (Gargiulo et al., 1999). It should be noted that, if a small strip of cytoplasm (containing ER membranes or mitochondria) is close to the plasma membrane, it can be

difficult to distinguish these localizations (see also Fig. 1E). In the context of our studies, the most relevant observation for ACSL1 is that it is intracellular yet capable of enhancing fatty acid uptake. This suggests that our findings have a general character, probably applying to both FATP and ACSL protein families and not just to FATP4.

Acyl-CoA synthetase activity decreases the intracellular concentration of fatty acids. Regardless of whether fatty acids translocate by themselves or with the help of proteins across the plasma membrane, a lowering of the intracellular fatty acid concentration will result in a corresponding increase of uptake as long as the extracellular concentration is high enough. Acyl-CoA synthetases would thus indirectly drive fatty acid uptake to maintain an equilibrium according to the law of mass action.

Another protein of the acyl-CoA synthetase family, the ER and mitochondria localized ACSL5, increased fatty acid uptake when overexpressed in a hepatocyte model cell line (Mashek et al., 2006). More evidence that the metabolic demand for fatty acids contributes to the extent of cellular fatty acid uptake has been reviewed recently (see Mashek and Coleman, 2006). However, defining conclusively the rate-limiting step under physiological conditions will still require dedicated future research.

The concept of vectorial acylation has been put forward as a model for long-chain fatty acid uptake in bacteria (Azizan et al., 1999; Klein et al., 1971). There, the bacterial fatty acid transporter FadL in the outer membrane works in concert with the inner-membrane-associated fatty acyl-CoA synthetase FadD. However, there is not even a remotely homologous protein to FadL in mammalian cells. It has been suggested that the yeast Fat1p protein (homologous to the mammalian FATP family) contains both transport and enzyme activity, and works in a complex with yeast acyl-CoA synthetases at the plasma membrane to drive fatty acid uptake by vectorial acylation (Black and DiRusso, 2003; Zou et al., 2002). Our results with the enzymatically dead S247A-FATP4 mutant show that the enhanced uptake of fatty acids is coupled to the acyl-CoA synthetase activity, implying that at least mammalian FATP4 does not contain an independent transport activity. The same has been observed for FATP1 (Stuhlsatz-Krouper et al., 1998).

To us, it makes a lot of sense to generate acyl-CoAs spatially close to where they are going to be used rather than at the plasma membrane. In this view, it is perhaps not at all surprising that FATP4 and possibly other acyl-CoAs are localized at the membrane of the ER. Acyl-CoA synthetases produced there can be directly used for the biosynthesis of phospholipids and triglycerides catalyzed by the ER-localized enzyme machinery. Mitochondrial acyl-CoA activity could preferentially provide activated fatty acids for the generation of energy via β-oxidation (Coleman et al., 2002). In recent years, putative fatty acid transporters have been the focus of much interest but it appears that a significant role for metabolic regulation of fatty acid uptake is gaining more acceptance now (Mashek and Coleman, 2006). The ER-localized acyl-CoA synthetase FATP4 is an important protein involved in these processes.

In conclusion, we suggest that spatial organization and expression of acyl-CoA synthetase activity is a key mechanism for both fatty acid uptake and utilization. It will be very interesting to follow how this concept will be integrated with the transport of fatty acids across the plasma membrane.

Materials and Methods

Antibodies

FATP4 antibodies were raised in rabbits according to standard procedures (Eurogentec, Seraing, Belgium) using the peptide corresponding to amino acids 629-643 of human FATP4 (DQEAYSRIQAGEEKL). Affinity purification of the antiserum against the peptide was as recommended by the manufacturer (Pierce, Rockford, IL). For peptide competition experiments, 1 μg of affinity-purified antibodies was pre-incubated with 10 μg of free peptide. Other antibodies used were rabbit anti-CaBP1 (Fullekrug et al., 1994), mouse anti-CD8 (OKT8) (Nickel et al., 1997); mouse anti-gp114 and p58 (canine CEACAM1 and β-Na^+K^+-ATPase, respectively) (Balcarova-Stander et al., 1984; Fullekrug et al., 2006); mouse anti-placenta alkaline phosphatase (PLAP) (DakoCytomation, Glostrup, Denmark), rabbit anti-calnexin (Dominguez et al., 1998), mouse anti-Na^+K^+-ATPase (Dianova, Germany), rabbit anti-PLAP (Verkade et al., 2000); mouse anti-Myc (9E10 hybridoma supernatant), mouse anti-FLAG (Sigma), Alexa Fluor 488 goat anti-rabbit (Invitrogen), Cy3 donkey anti-mouse/rabbit (Dianova, Hamburg, Germany).

Expression plasmids

All mutant FATP4 proteins and reporter constructs were generated by PCR and sequenced in both directions. Detailed cloning procedures are provided below, and oligonucleotide sequences are available in supplementary material Table 1. The N-terminus of LAT was amplified by PCR from lymphocyte cDNA. Tdimer2(12) (Campbell et al., 2002) was subcloned into pEGFP. PLAP cDNA (Brown et al., 1989) was P5D4 epitope-tagged and subcloned into pcDNA3 (T. Harder, University of Oxford, UK; personal communication). The following plasmids were used without modification: CaBP1 (Fullekrug et al., 1994), CD8 (Nilsson et al., 1989), ICAM-1-GFP (Barreiro et al., 2002), FLAG epitope-tagged ACSL1 (Kim et al., 2001), pOCT-GFP (Harder et al., 2004), plk16 (mito-RFP; containing the N-terminus of rat aldehyde dehydrogenase fused to RFP; gift of Christoph Thiele and Lars Kürschner, MPI Molecular Cell Biology, Dresden, Germany), lysozyme-Myc-KDEL (Lewis and Pelham, 1992).

FATP4.pcDNA3

Mouse cDNA (Herrmann et al., 2001) was amplified by PCR with primers sH3-F4wt (introducing *Hin*dIII and the Kozak sequence ACC in front of the starter ATG codon) and aF4wt. Subcloning into the mammalian expression vector pcDNA3 was with *Hin*dIII and *Xho*I.

ΔN-F4

This construct lacks the 46 N-terminal amino acids of the mmFATP4. Amplification of the new N-terminus was done by PCR using the primers sΔN-F4 and aF4-N*he*I.

FLAG-FATP4

The FLAG epitope (DYKDDDDK) was appended to the N-terminus of mouse FATP4 by PCR with primers sFLAG-F4 and aF4-*Nhe*I. The initiator methionine of the FATP4 cDNA was moved to the new N-terminus. The PCR product was digested with *Hin*dIII and *Nhe*I and replaced the corresponding fragment in the FATP4 expression plasmid.

F4-Nt-GFP

Domains of FATP4 and ACSL1 were defined using the Pfam database (Finn et al., 2006). All amino acids that are N-terminal of the region corresponding to PF00501 (AMP-binding enzyme) were used for the GFP-fusion proteins F4-Nt-GFP and A1-Nt-GFP. To construct F4-Nt-GFP we amplified the 5′ end of mouse FATP4 cDNA (nucleotides 1-306) using the sense primer s-H3-F4wt and the antisense primer a-THW-F4. These primers were chosen as to introduce a *Hin*dIII site at the 5′ end and an *Age*I site at the 3′ end. The PCR product was digested with *Hin*dIII and *Age*I and cloned into these sites in the pEGFP-N1 vector (Clontech, Mountain View, CA, USA).

A1-Nt-GFP

The ACSL1-GFP chimera contains the 66 N-terminal amino acids of rat ACSL1. PCR amplification using the primers sH3-ACS1 and aACS1-BamHI resulted in a fragment that was cloned into pEGFP-N1 using the newly introduced *Hin*dIII and *Bam*HI restriction sites.

LAT-GFP

The LAT-GFP chimera contains the 36 N-terminal amino acids of human LAT. The same construct has been described by Tanimura et al. (Tanimura et al., 2003). PCR amplification was done from lymphocyte cDNA using the primers sH3-LAT and aLAT-GFP. Cloning was done using the introduced *Hin*dIII and *Age*I sites and the pEGFP-N1 vector.

LAT-ERx-GFP

In the LAT-FATP4 chimera the N-terminus of LAT (amino acids 1-36) replaces the N-terminus of FATP4 (amino acids 1-46). A LAT-fragment was amplified using the primers sH3-LAT and a-LAT-wt. A FATP4 fragment was amplified using the 5′ primer LAT-F4, which contained the 21nt 3′ terminal of the LAT-fragment for annealing of the two fragments, and the 3′ primer aF4-NheI. The two fragments

were then ligated by PCR with the primers sH3-LAT and aF4-NheI. This product was digested with *Hin*dIII and *Nhe*I and replaced the 5′ of wt FATP4. Lat-ERx-GFP is a fusion protein of the 36 N-terminal amino acids of LAT, the ERx domain of FATP4 (amino acids 47-102) and the linker fragment to GFP (DPPVA).

It was created by using the LAT-FATP4 as template for a PCR with the primers sH3-LAT and aF4-wt. The product was digested with *Hin*dIII and *Bam*HI and cloned into these sites in the pEGFP-N1 vector.

S247A-FATP4

The S247A point mutation corresponds to the S250A mutant of FATP1 previously described (Stuhlsatz-Krouper et al., 1998). The S247A-FATP4 mutant was created using primers that contained the desired mutation as well as a silent restriction site for *Kpn*I. A 5′ fragment was amplified using the 5′ primer sH3-F4-wt and the 3′ primer aS247A-*Kpn*I, which introduced the desired mutation and the *Kpn*I site. The latter was complementary to the 5′ primer sS247A-*Kpn*I that was used for the 3′ fragment; the 3′ primer was aF4wt. Annealing of the two PCR fragments was by a third PCR using only the primers sH3-F4-wt and aF4wt. The product was digested with *Nhe*I and *Nde*I replacing this region in the wt FATP4 sequence. Insertion of the mutation was controlled by *Kpn*I digestion.

Immunofluorescence and immunohistochemistry

Selection of MDCK cells stably expressing FATP4-GFP with G-418 and epithelial polarization by cultivation on semipermeable Transwell filters (Corning Costar) for 4 days were as described previously (Meder et al., 2005).

COS-7 (ATCC CRL-1651), Vero (CCL-81), Ptk2 (CCL-56) and HeLa (CCL-2) cells were maintained under standard tissue culture conditions with the appropriate culture media. Cells grown to near confluency (10 cm^2) were transfected with 4 μg DNA and 10 μl lipofectamine 2000 (Invitrogen). Analysis was performed 24 hours after transfection. Immunofluorescence procedures (fixation with paraformaldehyde, permeabilization with 0.1% saponin), confocal image acquisition on a Leica TCS SP2 system and arrangement with Adobe Photoshop was as described earlier (Fullekrug et al., 1999). For luminal ER proteins, methanol (2 minutes at –20°C) was used instead of saponin for permeabilization (Fig. 1B, Fig. 2A, Fig. 5B,D). The confocal images shown in Figs 1, 2, 5-7 and supplementary material Fig. S1 are representative single sections.

Pieces of mouse small intestine were embedded in Tissue-Tek (Sakura Finetek, Tokyo, Japan) and flash frozen in liquid nitrogen. Cryosections were cut at 2 μm, and then processed for immunofluorescence as above, except that before mounting nuclei were stained with Hoechst 33342 (Invitrogen). Representative sections were chosen and projected (average intensity).

Subcellular fractionation

HeLa cells from three 165 cm^2 petri dishes were collected and resuspended in 2 ml of KT buffer (130 mM KCl, 25 mM Tris-HCl, pH 7.5). Homogenization was by repeated passing through needles (5× 22G, 5× 25G). Postnuclear supernatant (PNS) (1.5 ml) obtained after 5 minutes of centrifugation at 1000 ***g*** was layered on top of an Optiprep step gradient (from bottom to top: 0.67 ml 40%, 1.33 ml each of 20%, 15%, 12.5%, 10%, 7.5%, 5%, 2.5% Optiprep in KT buffer). After centrifugation for 30 minutes at 66,000 ***g*** in a SW41 rotor, nine fractions were collected from top to bottom. Each fraction was diluted 1:1 with KT buffer, and membranes were sedimented in a TLA45 rotor at 100,000 ***g*** for 60 minutes.

Glycosylation analysis

The N-terminus of FATP4 was extended with a glycosylation tag from human rhodopsin (MNGTEGPNFYVPFSNAT) (Bulbarelli et al., 2002) by PCR with primers s-ops-F4 and aF4-*Nhe*I (see supplementary material Table 1). Underlined amino acids refer to the consensus site for N-glycosylation (N-X-S/T). The PCR product was digested with *Hin*dIII and *Nhe*I and replaced the corresponding 5′ region of wt FATP4.

Ops-ctrl

Two asparagine residues of opsinF4 were changed to glutamine, thus destroying the consensus sites for N-glycosylation. PCR was with primers s-octr-F4 and aF4-NheI and cloning was as for opsinF4. Level of expression, localization, B_{12}-FA uptake and ACS activity were not significantly changed when compared with wt FATP4.

HeLa cells were transiently transfected with plasmids opsinF4 and ops-ctrl coding for FATP4 with or without an N-terminal glycosylation tag. Total membranes (5×10^5 cells) were prepared by centrifugation of a PNS at 100,000 ***g*** for 60 minutes. The pellet was heated for 5 minutes at 95°C in 150 μl of buffer H (150 mM sodium citrate, pH 5.5, 0.6% SDS, 1.6% v/v β-mercaptoethanol). After cooling, SDS was quenched by addition of 300 μl 0.75% NP-40, and the mixture was heated again at 95°C for 1 minute. After cooling and addition of proteinase inhibitor cocktail, the solution was split in two aliquots (±5 mU EndoH; Roche Diagnostics, Mannheim, Germany). Incubation was overnight at 37°C followed by protein precipitation and SDS-PAGE analysis.

B_{12}-FA uptake and FACS analysis

Flow cytometric analysis on a Becton Dickinson FACSCalibur was essentially performed as described (Schaffer and Lodish, 1994). Transfected COS cells were washed twice with PBS++ (PBS containing 0.9 mM $CaCl_2$, 0.5 mM $MgCl_2$) and then incubated with 2 μM B_{12}-FA [Bodipy 3823 (4,4-difluoro-5,7-diphenyl-4-bora-3a,4a-diaza-*s*-indacene-3-dodecanoic acid) Invitrogen] bovine serum albumin (BSA) solution. Fatty acid uptake was terminated after 2 minutes by adding ice-cold 0.1% BSA in PBS. After trypsinization, cells were fixed in suspension by 4% paraformaldehyde for 15 minutes. Appropriate controls (for autofluorescence, single signals) were used for calibration of the FACS analysis. Data were exported from the CellQuestPro software (BD Biosciences, San Jose, CA) and analyzed by spreadsheet calculations (Tzircotis et al., 2004). Each data point in Fig. 8A contains all cells with the same fluorescence value of tdimer (equals the level of expression) and the average B_{12}-FA fluorescence of these cells (equals the amount of fatty acid taken up).

For the qualitative analysis of fatty acid uptake, 20 μM of B_{12}-FA was used and the cells were fixed after two washes with ice-cold 0.1% BSA in PBS.

For the surface quantification of FLAG-FATP4, COS cells were detached with 5 mM EDTA in PBS instead of trypsin. Cells were divided into aliquots of 7×10^5 cells, resuspended in FACS buffer (0.5% w/v BSA, 0.05% sodium azide, 5 mM EDTA in PBS) and stained with mouse anti-FLAG and rabbit anti-FATP4 antibodies for 30 minutes on ice followed by secondary antibodies [anti-mouse Cy2 and anti-rabbit phycoerythrin (PE)]; appropriate washing steps were by pelleting and resuspension. For internal staining, cells were fixed for 20 minutes with paraformaldehyde, washed and permeabilized with 0.1% TX-100 for 5 minutes. For proper FACS settings, controls included transfected cells without primary antibodies, single stainings of permeabilized cells (maximum Cy2 or PE signal) and cells not expressing the FLAG epitope (unspecific binding of FLAG antibody). In the representative experiment shown in Fig. 4D, 10^4 cells were analyzed; no cells were found to display a surface staining for FLAG. In a different experiment, we counted 10^5 cells and found three cells corresponding to 0.02% of all FLAG-FATP4-expressing cells; this was not considered significant.

Acyl-CoA synthetase activity

The protocol according to Hall et al. (Hall et al., 2003) was used with slight modifications. Briefly, cells were lysed for 30 minutes on ice with 1% TX-100, 130 mM KCl, 25 mM Tris-HCl, pH 7.4. Lysates containing 20-30 μg of total protein were incubated for 10 minutes at 30°C in 100 mM Tris, pH 7.4, 5 mM $MgCl_2$, 200 μM dithiothreitol (DTT), 10 mM ATP, 0.2% TX-100, 20 μM [^{3}H]oleate (specific activity 10 Ci/mol), 200 μM CoA. After stopping with Dole's solution (isopropanol: n-heptane: H_2SO_4 40:10:1), unreacted oleate was extracted four times with n-heptane, and the remaining oleoyl-CoA in the aqueous phase determined by scintillation counting. In pilot experiments it was determined that ACSL1 and endogenous ACS activity increased when TX-100 was used for solubilization. FATP4 activity was decreased, however. The 0.2% final concentration of TX-100 chosen is a compromise between these opposing effects. This cautions against a quantitative comparison of the activities determined.

The expression of wt FATP4 and S247A FATP4 was compared by western blotting and found not to differ significantly.

Oleate uptake

Cumulative uptake of oleate was based on Stremmel and Berk (Stremmel and Berk, 1986). Adherent cells were incubated for 5 minutes at 37°C with ^{3}H-oleate uptake solution (170 μM [^{3}H]oleate, 170 μM BSA in PBS; specific activity 4.1 Ci/mol). After stopping and washing with ice-cold 0.5% BSA in PBS, cells were lysed with 1 M NaOH and aliquots analyzed for protein concentration and radioactivity by scintillation counting.

Thin-layer chromatography

Following the oleate uptake assay, lipids were extracted according to Folch et al. (Folch et al., 1957), with the modification that the water phase was acidified by 50 mM citric acid. Only background radioactivity was found in the aqueous phase. The organic phase was vacuum dried, resolubilized in chloroform:methanol 1:2 and spotted onto silica gel 60 plates (Merck). The running solvent was chloroform:ethanol:water:triethylamine 35:40:9:35 (Kuerschner et al., 2004). This particular mixture was chosen because free oleate is very well separated from phospholipids and neutral lipids. Retention factors (Rf) of commercial standards were: sphingomyelin (0.06), phosphatidylcholine (0.09), phosphatidylserine (0.10), phosphatidylinositol (0.22), phosphatidylethanolamine (0.29), oleate (0.55), monoolein (0.66), diolein (0.82), cholesteryl oleate (0.84) and triolein (0.84). For quantification, the following subclasses were defined: phospholipids (Rf 0.02-0.33), not identified (Rf 0.34-0.51), oleate (Rf 0.52-0.59) and neutral lipids (Rf 0.62-0.88). After iodine staining, areas were scraped and quantified by scintillation counting.

Localization of ACSL1

The localization of ACSL1 to mitochondria as shown for epithelial-like Ptk2 cells (Fig. 6A) and COS cells (Fig. 7B) was also observed in epitheloid HeLa, hepatocyte-like WIF-B and epithelial-like Vero cells (data not shown). In highly overexpressing COS cells, ACSL1 was also found partially at the ER (supplementary material Fig. S1). Immunofluorescence tends to overemphasize concentrated (e.g. mitochondria)

over widely distributed or diluted labeling (e.g. ER, cytoplasm). As such, it cannot be concluded from our experiments that there is no ACSL1 in the ER at all. Nevertheless, the mitochondrial localization is striking (Fig. 6A, Fig. 7B) and it is difficult to imagine that there should be no physiological correlation to this. That there is mitochondrial targeting information in the N-terminus of ACSL1 is already shown in Fig. 6B. Furthermore, the N-terminus of ACSL1 is also sufficient to direct an ACSL1-FATP4 fusion protein to mitochondria (data not shown).

As mentioned before, ACSL1 has been localized to the plasma membrane of adipocytes by immunofluorescence (Gargiulo et al., 1999) and the ER and mitochondria-associated membrane by subcellular fractionation of rat liver (Lewin et al., 2001). Furthermore, in a proteomics approach, ACSL1 was found on the lipid droplets of adipocytes (Brasaemle et al., 2004). In summary, the weakness of all studies (including ours) is that only one particular technique was used on one particular model system. Hopefully future studies will be more comprehensive to localize ACSL1, especially regarding possible cell-specific differences in distribution.

We thank Isabella Gosch, Richard Sparla, Simone Staffer and Sabine Tuma for expert technical assistance. David Bernlohr (University of Minnesota, USA) provided initial help with the ACS assay. Francisco Sánchez-Madrid (Universidad Autonoma de Madrid, Spain), Rosalind Coleman (University of North Carolina, USA), Heidi McBride (University of Ottawa, Canada), Roger Tsien (University of California at San Diego, USA) and Christoph Thiele (MPI Molecular Cell Biology, Germany) kindly supplied expression plasmids crucial for this study. We thank Leica Microsystems for continuous support of the Advanced Light Microscopy Facility at EMBL, Heidelberg, and Günther Giese at the microscopy facility of the MPI for Medical Research, Heidelberg. Dieter Stefan helped with the FACS analysis at the Institute of Immunology, Heidelberg. We would like to give special thanks to Kai Simons for critically reading the manuscript. This work was supported by a grant of the Dietmar Hopp Foundation (to W.S.), by the Stiftung Nephrologie (to R.E. and J.F.) and by NIH grant NS37355 (to P.A.W.).

References

Azizan, A., Sherin, D., DiRusso, C. C. and Black, P. N. (1999). Energetics underlying the process of long-chain fatty acid transport. *Arch. Biochem. Biophys.* **365**, 299-306.

Balcarova-Stander, J., Pfeiffer, S. E., Fuller, S. D. and Simons, K. (1984). Development of cell surface polarity in the epithelial Madin-Darby canine kidney (MDCK) cell line. *EMBO J.* **3**, 2687-2694.

Barreiro, O., Yanez-Mo, M., Serrador, J. M., Montoya, M. C., Vicente-Manzanares, M., Tejedor, R., Furthmayr, H. and Sanchez-Madrid, F. (2002). Dynamic interaction of VCAM-1 and ICAM-1 with moesin and ezrin in a novel endothelial docking structure for adherent leukocytes. *J. Cell Biol.* **157**, 1233-1245.

Black, P. N. and DiRusso, C. C. (2003). Transmembrane movement of exogenous long-chain fatty acids: proteins, enzymes, and vectorial esterification. *Microbiol. Mol. Biol. Rev.* **67**, 454-472.

Bonen, A., Luiken, J. J. and Glatz, J. F. (2002). Regulation of fatty acid transport and membrane transporters in health and disease. *Mol. Cell. Biochem.* **239**, 181-192.

Brasaemle, D. L., Dolios, G., Shapiro, L. and Wang, R. (2004). Proteomic analysis of proteins associated with lipid droplets of basal and lipolytically-stimulated 3T3-L1 adipocytes. *J. Biol. Chem.* **279**, 46835-46842.

Bray, G. A. and Tartaglia, L. A. (2000). Medicinal strategies in the treatment of obesity. *Nature* **404**, 672-677.

Brown, D. A., Crise, B. and Rose, J. K. (1989). Mechanism of membrane anchoring affects polarized expression of two proteins in MDCK cells. *Science* **245**, 1499-1501.

Bulbarelli, A., Sprocati, T., Barberi, M., Pedrazzini, E. and Borgese, N. (2002). Trafficking of tail-anchored proteins: transport from the endoplasmic reticulum to the plasma membrane and sorting between surface domains in polarised epithelial cells. *J. Cell Sci.* **115**, 1689-1702.

Campbell, R. E., Tour, O., Palmer, A. E., Steinbach, P. A., Baird, G. S., Zacharias, D. A. and Tsien, R. Y. (2002). A monomeric red fluorescent protein. *Proc. Natl. Acad. Sci. USA* **99**, 7877-7882.

Coe, N. R., Smith, A. J., Frohnert, B. I., Watkins, P. A. and Bernlohr, D. A. (1999). The fatty acid transport protein (FATP1) is a very long chain acyl-CoA synthetase. *J. Biol. Chem.* **274**, 36300-36304.

Coleman, R. A., Lewin, T. M. and Muoio, D. M. (2000). Physiological and nutritional regulation of enzymes of triacylglycerol synthesis. *Annu. Rev. Nutr.* **20**, 77-103.

Coleman, R. A., Lewin, T. M., Van Horn, C. G. and Gonzalez-Baro, M. R. (2002). Do long-chain Acyl-CoA synthetases regulate fatty acid entry into synthetic versus degradative pathways? *J. Nutr.* **132**, 2123-2126.

Dominguez, M., Dejgaard, K., Fullekrug, J., Dahan, S., Fazel, A., Paccaud, J.-P., Thomas, D. Y., Bergeron, J. J. M. and Nilsson, T. (1998). gp25L/emp24/p24 protein family members of the cis-Golgi network bind both COP I and II coatomer. *J. Cell Biol.* **140**, 751-765.

Finn, R. D., Mistry, J., Schuster-Bockler, B., Griffiths-Jones, S., Hollich, V., Lassmann, T., Moxon, S., Marshall, M., Khanna, A., Durbin, R. et al. (2006). Pfam: clans, web tools and services. *Nucleic Acids Res.* **34**, D247-D251.

Folch, J., Lees, M. and Sloane Stanley, G. H. (1957). A simple method for the isolation and purification of total lipides from animal tissues. *J. Biol. Chem.* **226**, 497-509.

Fullekrug, J., Sonnichsen, B., Wunsch, U., Arseven, K., Nguyen Van, P., Soling, H. and Mieskes, G. (1994). CaBP1, a calcium binding protein of the thioredoxin family, is a resident KDEL protein of the ER and not of the intermediate compartment. *J. Cell Sci.* **107**, 2719-2727.

Fullekrug, J., Scheiffele, P. and Simons, K. (1999). VIP36 localisation to the early secretory pathway. *J. Cell Sci.* **112**, 2813-2821.

Fullekrug, J., Shevchenko, A., Shevchenko, A. and Simons, K. (2006). Identification of glycosylated marker proteins of epithelial polarity in MDCK cells by homology driven proteomics. *BMC Biochem.* **7**, 8.

Garcia-Martinez, C., Marotta, M., Moore-Carrasco, R., Guitart, M., Camps, M., Busquets, S., Montell, E. and Gomez-Foix, A. M. (2005). Impact on fatty acid metabolism and differential localization of FATP1 and FAT/CD36 proteins delivered in cultured human muscle cells. *Am. J. Physiol. Cell Physiol.* **288**, C1264-C1272.

Gargiulo, C. E., Stuhlsatz-Krouper, S. M. and Schaffer, J. E. (1999). Localization of adipocyte long-chain fatty acyl-CoA synthetase at the plasma membrane. *J. Lipid Res.* **40**, 881-892.

Gimeno, R. E., Hirsch, D. J., Punreddy, S., Sun, Y., Ortegon, A. M., Wu, H., Daniels, T., Stricker-Krongrad, A., Lodish, H. F. and Stahl, A. (2003). Targeted deletion of fatty acid transport protein-4 results in early embryonic lethality. *J. Biol. Chem.* **278**, 49512-49516.

Guo, W., Huang, N., Cai, J., Xie, W. and Hamilton, J. A. (2005). Fatty acid transport and metabolism in HepG2 cells. *Am. J. Physiol. Gastrointest. Liver Physiol.* **290**, G528-G534.

Hajri, T. and Abumrad, N. A. (2002). Fatty acid transport across membranes: relevance to nutrition and metabolic pathology. *Annu. Rev. Nutr.* **22**, 383-415.

Hall, A. M., Smith, A. J. and Bernlohr, D. A. (2003). Characterization of the Acyl-CoA synthetase activity of purified murine fatty acid transport protein 1. *J. Biol. Chem.* **278**, 43008-43013.

Hall, A. M., Wiczer, B. M., Herrmann, T., Stremmel, W. and Bernlohr, D. A. (2005). Enzymatic properties of purified murine fatty acid transport protein 4 and analysis of Acyl CoA synthetase activities in tissues from FATP4 null mice. *J. Biol. Chem.* **280**, 11948-11954.

Hamilton, J. and Kamp, F. (1999). How are free fatty acids transported in membranes? Is it by proteins or by free diffusion through the lipids? *Diabetes* **48**, 2255-2269.

Hamilton, J. A., Guo, W. and Kamp, F. (2002). Mechanism of cellular uptake of long-chain fatty acids: do we need cellular proteins? *Mol. Cell. Biochem.* **239**, 17-23.

Harder, Z., Zunino, R. and McBride, H. (2004). Sumo1 conjugates mitochondrial substrates and participates in mitochondrial fission. *Curr. Biol.* **14**, 340-345.

Hartmann, E., Rapoport, T. A. and Lodish, H. F. (1989). Predicting the orientation of eukaryotic membrane-spanning proteins. *Proc. Natl. Acad. Sci. USA* **86**, 5786-5790.

Herrmann, T., Buchkremer, F., Gosch, I., Hall, A. M., Bernlohr, D. A. and Stremmel, W. (2001). Mouse fatty acid transport protein 4 (FATP4): characterization of the gene and functional assessment as a very long chain acyl-CoA synthetase. *Gene* **270**, 31-40.

Herrmann, T., van der Hoeven, F., Grone, H. J., Stewart, A. F., Langbein, L., Kaiser, I., Liebisch, G., Gosch, I., Buchkremer, F., Drobnik, W. et al. (2003). Mice with targeted disruption of the fatty acid transport protein 4 (Fatp **4**, Slc27a4) gene show features of lethal restrictive dermopathy. *J. Cell Biol.* **161**, 1105-1115.

Higy, M., Junne, T. and Spiess, M. (2004). Topogenesis of membrane proteins at the endoplasmic reticulum. *Biochemistry* **43**, 12716-12722.

Hirsch, D., Stahl, A. and Lodish, H. F. (1998). A family of fatty acid transporters conserved from mycobacterium to man. *Proc. Natl. Acad. Sci. USA* **95**, 8625-8629.

Kalant, D. and Cianflone, K. (2004). Regulation of fatty acid transport. *Curr. Opin. Lipidol.* **15**, 309-314.

Kim, J.-H., Lewin, T. M. and Coleman, R. A. (2001). Expression and characterization of recombinant Rat Acyl-CoA synthetases 1, 4, and 5: selective inhibition by triacsin c and thiazolidinediones. *J. Biol. Chem.* **276**, 24667-24673.

Klein, K., Steinberg, R., Fiethen, B. and Overath, P. (1971). Fatty acid degradation in Escherichia coli. An inducible system for the uptake of fatty acids and further characterization of old mutants. *Eur. J. Biochem.* **19**, 442-450.

Kuerschner, L., Ejsing, C. S., Ekroos, K., Shevchenko, A., Anderson, K. I. and Thiele, C. (2004). Polyene-lipids: a new tool to image lipids. *Nat. Methods* **2**, 39-45.

Lewin, T. M., Kim, J.-H., Granger, D. A., Vance, J. E. and Coleman, R. A. (2001). Acyl-CoA synthetase isoforms 1, 4, and 5 are present in different subcellular membranes in rat liver and can be inhibited independently. *J. Biol. Chem.* **276**, 24674-24679.

Lewis, M. J. and Pelham, H. R. (1992). Ligand-induced redistribution of a human KDEL receptor from the Golgi complex to the endoplasmic reticulum. *Cell* **68**, 353-364.

Lewis, S. E., Listenberger, L. L., Ory, D. S. and Schaffer, J. E. (2001). Membrane topology of the murine fatty acid transport protein 1. *J. Biol. Chem.* **276**, 37042-37050.

Luetterforst, R., Stang, E., Zorzi, N., Carozzi, A., Way, M. and Parton, R. G. (1999). Molecular characterization of caveolin association with the golgi complex: identification of a cis-golgi targeting domain in the caveolin molecule. *J. Cell Biol.* **145**, 1443-1459.

Mashek, D. G. and Coleman, R. A. (2006). Cellular fatty acid uptake: the contribution of metabolism. *Curr. Opin. Lipidol.* **17**, 274-278.

Mashek, D. G., McKenzie, M. A., Van Horn, C. G. and Coleman, R. A. (2006). Rat long chain Acyl-CoA synthetase 5 increases fatty acid uptake and partitioning to cellular triacylglycerol in McArdle-RH7777 cells. *J. Biol. Chem.* **281**, 945-950.

Meder, D., Shevchenko, A., Simons, K. and Fullekrug, J. (2005). Gp135/podocalyxin and NHERF-2 participate in the formation of a preapical domain during polarization of MDCK cells. *J. Cell Biol.* **168**, 303-313.

Moulson, C. L., Martin, D. R., Lugus, J. J., Schaffer, J. E., Lind, A. C. and Miner, J. H. (2003). Cloning of wrinkle-free, a previously uncharacterized mouse mutation, reveals crucial roles for fatty acid transport protein 4 in skin and hair development. *Proc. Natl. Acad. Sci. USA* **100**, 5274-5279.

Nickel, W., Sohn, K., Bunning, C. and Wieland, F. T. (1997). p23, a major COPI-vesicle membrane protein, constitutively cycles through the early secretory pathway. *Proc. Natl. Acad. Sci. USA* **94**, 11393-11398.

Nilsson, T., Jackson, M. and Peterson, P. A. (1989). Short cytoplasmic sequences serve as retention signals for transmembrane proteins in the endoplasmic reticulum. *Cell* **58**, 707-718.

Pei, Z., Fraisl, P., Berger, J., Jia, Z., Forss-Petter, S. and Watkins, P. A. (2004). Mouse very long-chain Acyl-CoA synthetase 3/fatty acid transport protein 3 catalyzes fatty acid activation but not fatty acid transport in MA-10 cells. *J. Biol. Chem.* **279**, 54454-54462.

Pohl, J., Ring, A. and Stremmel, W. (2002). Uptake of long-chain fatty acids in HepG2 cells involves caveolae: analysis of a novel pathway. *J. Lipid Res.* **43**, 1390-1399.

Schaffer, J. E. and Lodish, H. F. (1994). Expression cloning and characterization of a novel adipocyte long chain fatty acid transport protein. *Cell* **79**, 427-436.

Stahl, A., Hirsch, D. J., Gimeno, R. E., Punreddy, S., Ge, P., Watson, N., Patel, S., Kotler, M., Raimondi, A., Tartaglia, L. A. et al. (1999). Identification of the major intestinal fatty acid transport protein. *Mol. Cell* **4**, 299-308.

Stahl, A., Gimeno, R. E., Tartaglia, L. A. and Lodish, H. F. (2001). Fatty acid transport proteins: a current view of a growing family. *Trends Endocrinol. Metab.* **12**, 266-273.

Steinberg, S. J., Wang, S. J., Kim, D. G., Mihalik, S. J. and Watkins, P. A. (1999a). Human very-long-chain acyl-CoA synthetase: cloning, topography, and relevance to branched-chain fatty acid metabolism. *Biochem. Biophys. Res. Commun.* **257**, 615-621.

Steinberg, S. J., Wang, S. J., McGuinness, M. C. and Watkins, P. A. (1999b). Human liver-specific very-long-chain Acyl-coenzyme a synthetase: cDNA cloning and characterization of a second enzymatically active protein. *Mol. Genet. Metab.* **68**, 32-42.

Stremmel, W. and Berk, P. D. (1986). Hepatocellular influx of [14C]oleate reflects membrane transport rather than intracellular metabolism or binding. *Proc. Natl. Acad. Sci. USA* **83**, 3086-3090.

Stremmel, W., Pohl, L., Ring, A. and Herrmann, T. (2001). A new concept of cellular uptake and intracellular trafficking of long-chain fatty acids. *Lipids* **36**, 981-989.

Stuhlsatz-Krouper, S. M., Bennett, N. E. and Schaffer, J. E. (1998). Substitution of alanine for serine 250 in the murine fatty acid transport protein inhibits long chain fatty acid transport. *J. Biol. Chem.* **273**, 28642-28650.

Tanimura, N., Nagafuku, M., Minaki, Y., Umeda, Y., Hayashi, F., Sakakura, J., Kato, A., Liddicoat, D. R., Ogata, M., Hamaoka, T. et al. (2003). Dynamic changes in the mobility of LAT in aggregated lipid rafts upon T cell activation. *J. Cell Biol.* **160**, 125-135.

Tzircotis, G., Thorne, R. F. and Isacke, C. M. (2004). A new spreadsheet method for the analysis of bivariate flow cytometric data. *BMC Cell Biol.* **5**, 10.

Verkade, P., Harder, T., Lafont, F. and Simons, K. (2000). Induction of caveolae in the apical plasma membrane of Madin-Darby canine kidney cells. *J. Cell Biol.* **148**, 727-739.

von Heijne, G. (1989). Control of topology and mode of assembly of a polytopic membrane protein by positively charged residues. *Nature* **341**, 456-458.

Watkins, P. A., Pevsner, J. and Steinberg, S. J. (1999). Human very long-chain acyl-CoA synthetase and two human homologs: initial characterization and relationship to fatty acid transport protein. *Prostaglandins Leukot. Essent. Fatty Acids* **60**, 323-328.

Zakim, D. (2000). Thermodynamics of fatty acid transfer. *J. Membr. Biol.* **176**, 101-109.

Zou, Z., DiRusso, C. C., Ctrnacta, V. and Black, P. N. (2002). Fatty acid transport in Saccharomyces cerevisiae. Directed mutagenesis of FAT1 distinguishes the biochemical activities associated with Fat1p. *J. Biol. Chem.* **277**, 31062-31071.